

Supporting information for "Impact of updating vegetation information on land surface model performance"

Melissa Ruiz-Vásquez^{1,2}, Sungmin O³, Gabriele Arduini⁴, Souhail Boussetta⁴, Alexander Brenning², Ana Bastos¹, Sujan Koirala¹, Gianpaolo Balsamo⁴, Markus Reichstein¹, and René Orth¹

¹Department of Biogeochemical Integration, Max Planck Institute for Biogeochemistry, Jena, Germany

²Friedrich Schiller University Jena, Department of Geography, Jena, Germany

³Department of Climate and Energy System Engineering, Ewha Womans University, Seoul, South Korea

⁴Research Department, European Centre for Medium-Range Weather Forecasts, Reading, UK

Contents of this file	Page
1. Table S1.	3
2. Figure S1.	4
3. Figure S2.	5
4. Figure S3.	6
5. Figure S4.	7
6. Figure S5.	8

Corresponding author: M. Ruiz-Vásquez, Department of Biogeochemical Integration, Max Planck Institute for Biogeochemistry, Jena, Germany (mruiz@bgc-jena.mpg.de)

7. Figure S6.	9
8. Figure S7.	10
9. Figure S8.	11
10. Figure S9.	12
11. Figure S10.	13
12. Figure S11.	14

Introduction

The present document contains additional material (Table and Figures) that supports the discussion in the study "Impact of updating vegetation information on land surface model performance". This material is not included in the main text because it is not essential to the main scientific conclusions other than providing additional information.

Table S1. Optimal perturbation factors for the model parameters after global calibration

Model parameter	Optimal perturbation factors
Hydraulic conductivity	0.09766
Humidity stress function	0.83900
Minimum stomatal resistance	1.27800
Soil moisture stress function	1.47000
Total soil depth	1.06044
Transmission of net solar radiation through vegetation	0.13652

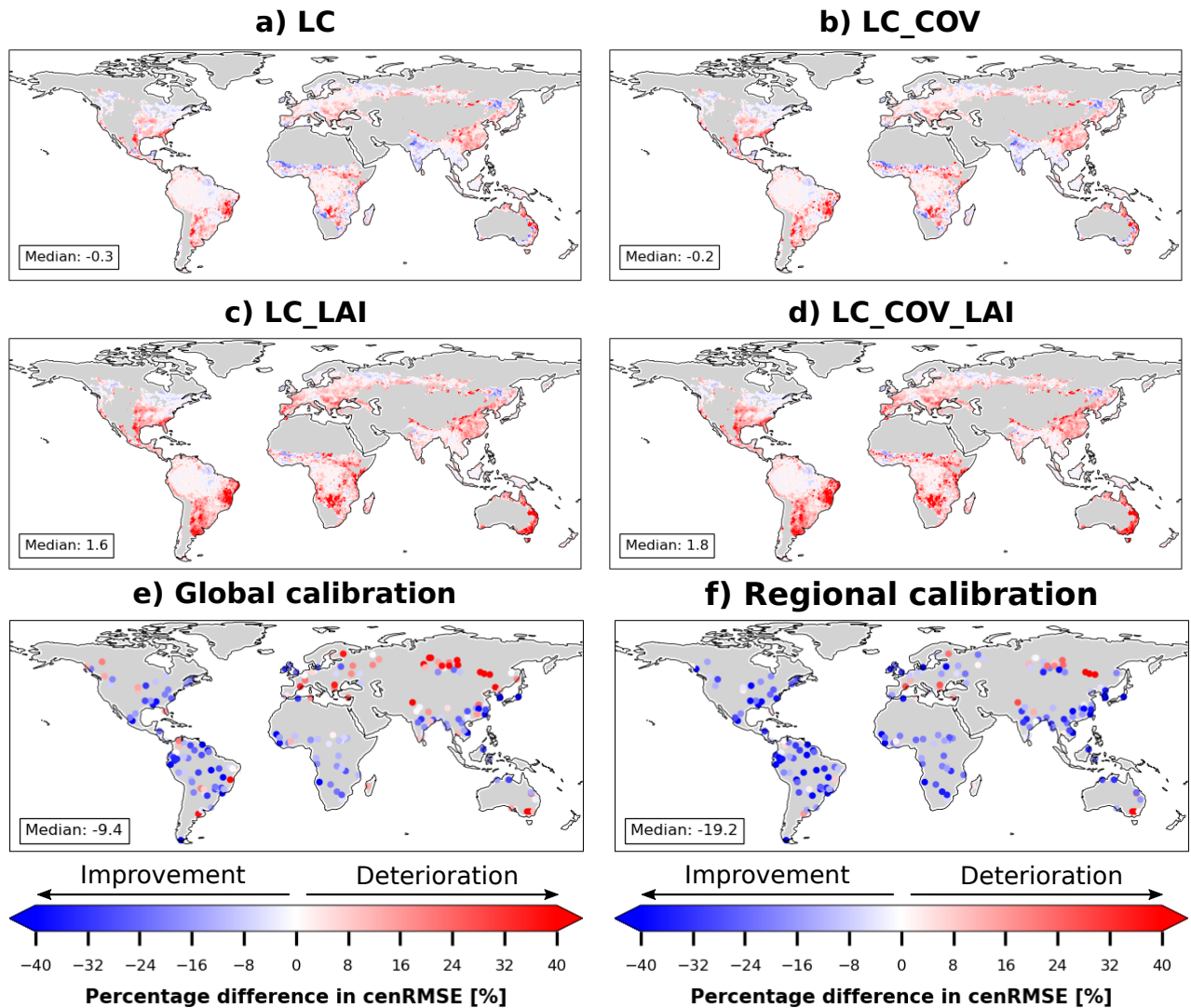


Figure S1. Percentage differences in cenRMSE model performance for near-surface soil moisture in a) LC, b) LC_COV, c) LC_LAI, d) LC_COV_LAI, e) Global calibration and f) Regional calibration simulations with regards to CONTROL simulation. Numbers in the textboxes represent the global median.

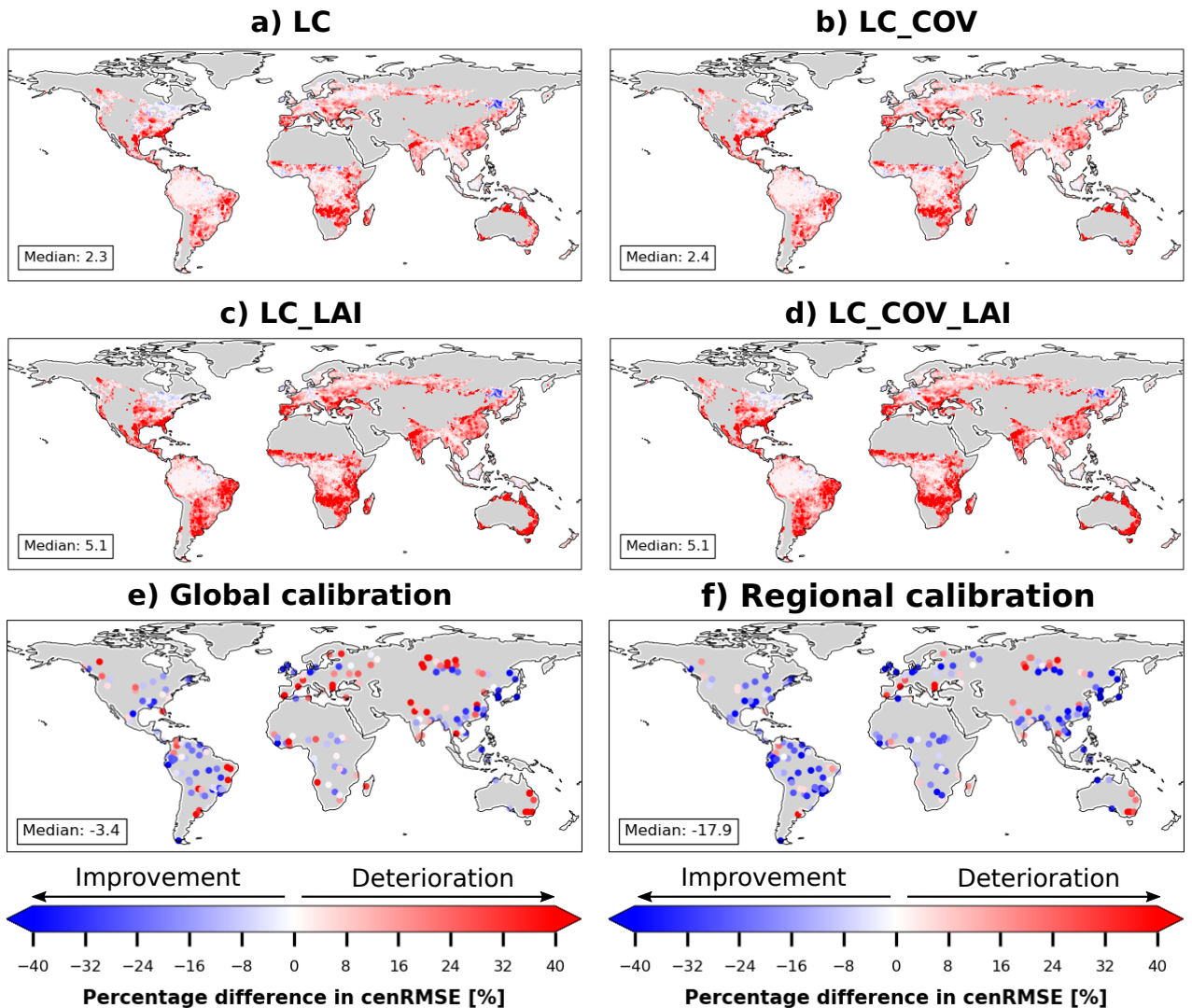


Figure S2. Similar to Figure S1, but for deep soil moisture.

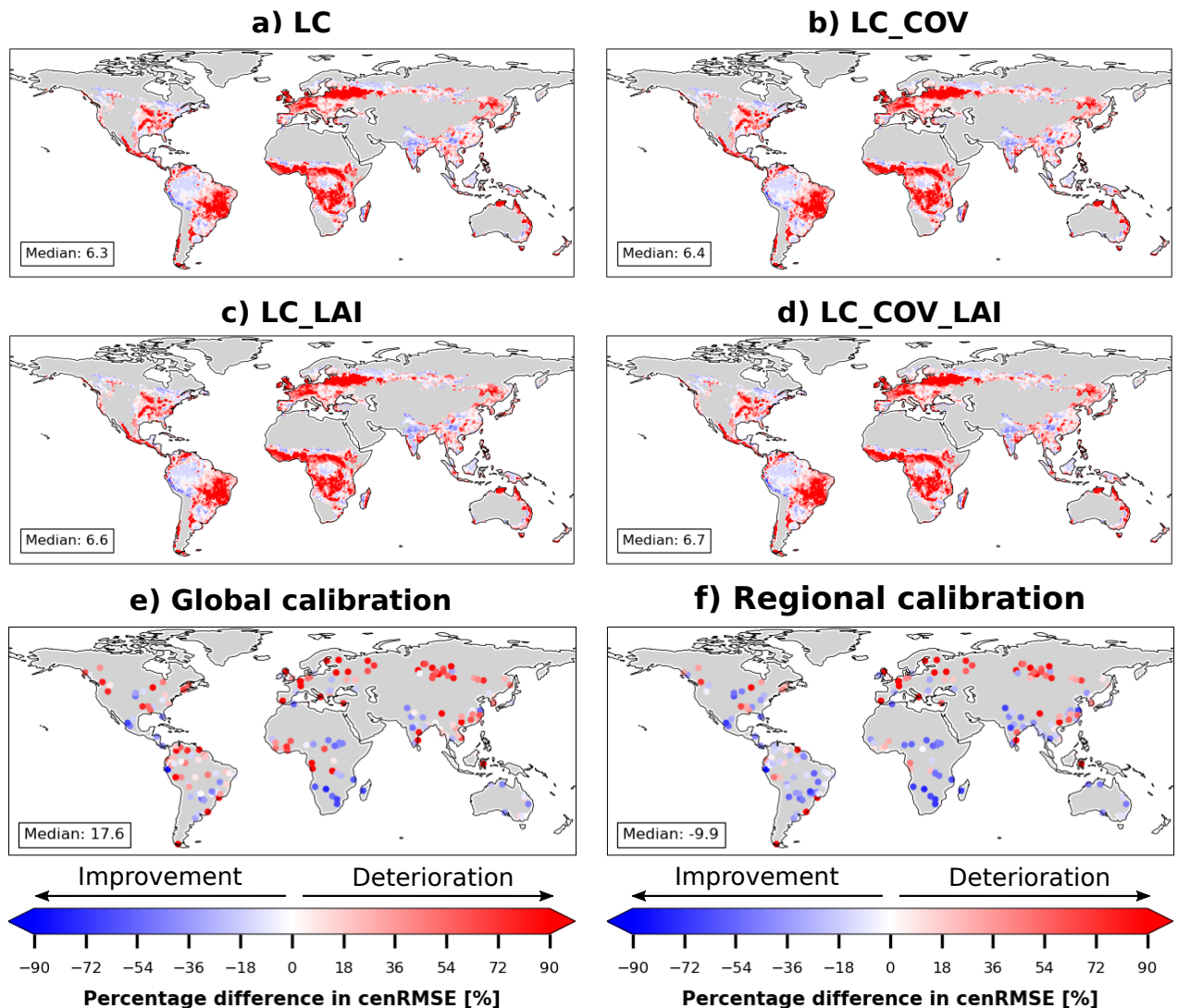


Figure S3. Similar to Figure S1, but for surface latent heat flux.

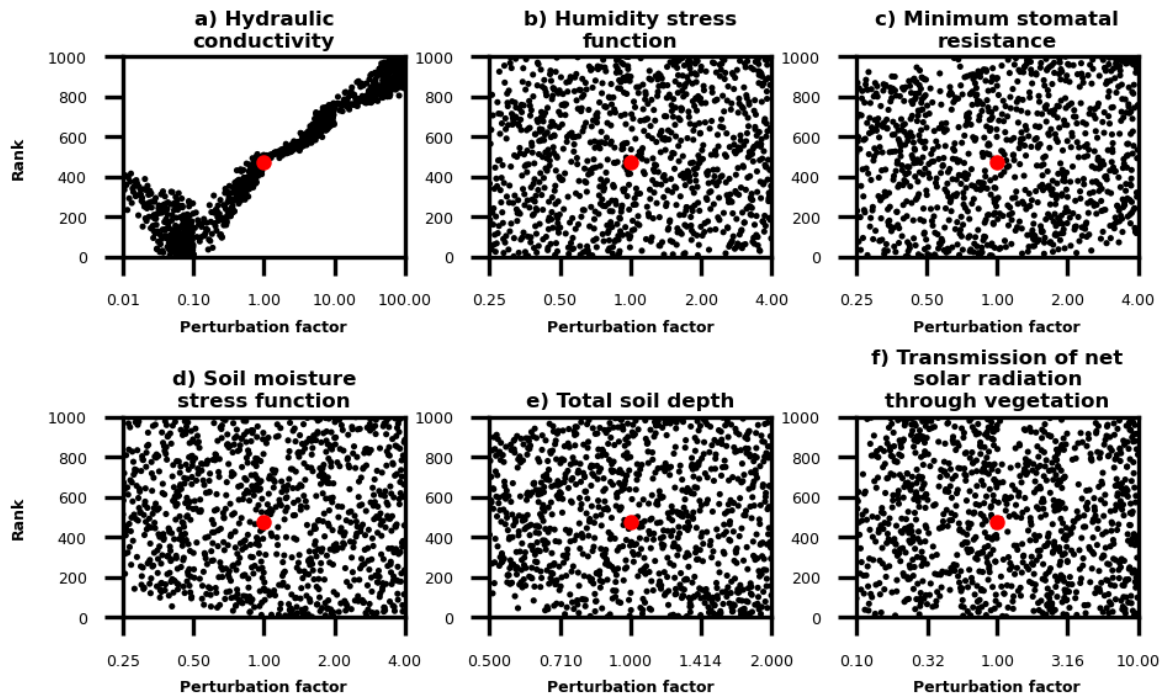


Figure S4. Rankings of 1001 random perturbation factors for near-surface soil moisture for a) hydraulic conductivity, b) humidity stress function, c) minimum stomatal resistance, d) soil moisture stress function, e) total soil depth and f) transmission of net solar radiation through vegetation. Red dots indicate the performance of the default parameterizations (i.e. no perturbation).

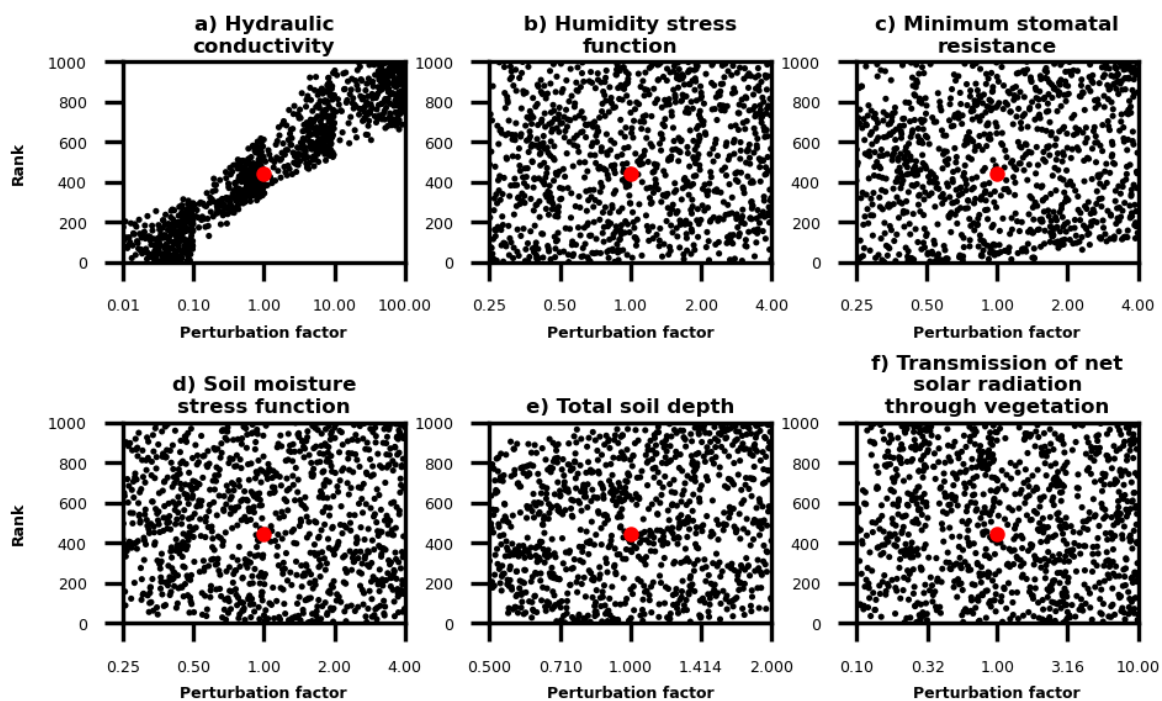


Figure S5. Similar to Figure S4, but for deep soil moisture.

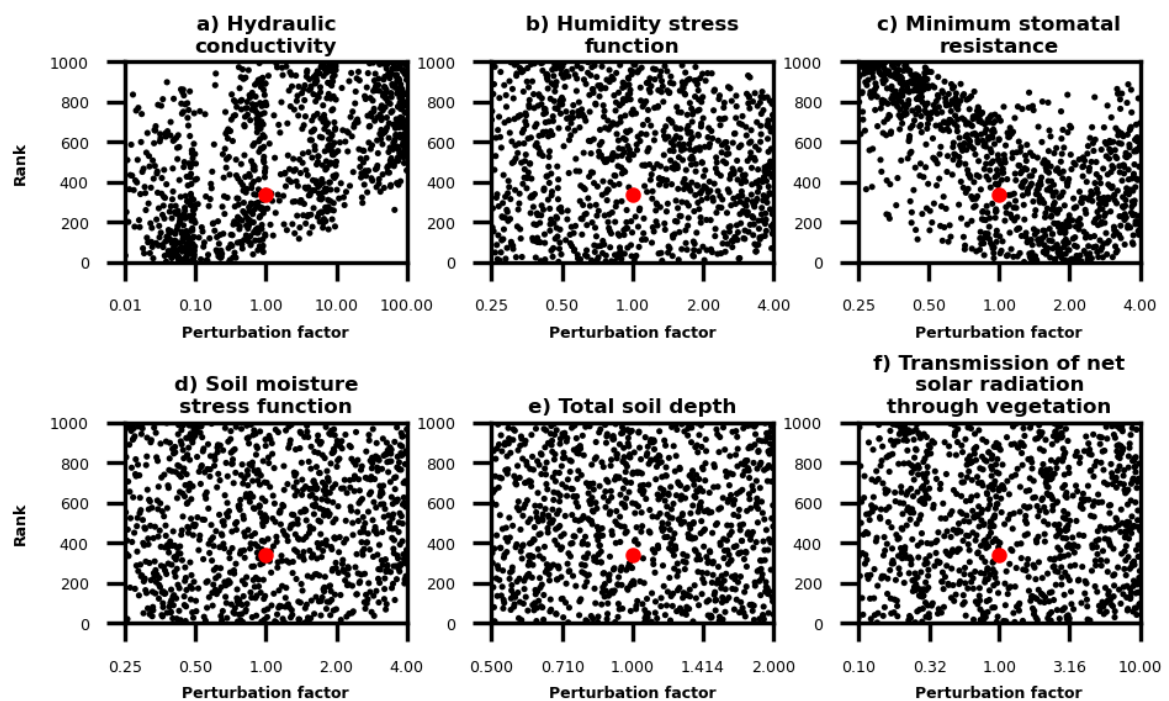


Figure S6. Similar to Figure S4, but for surface latent heat flux.

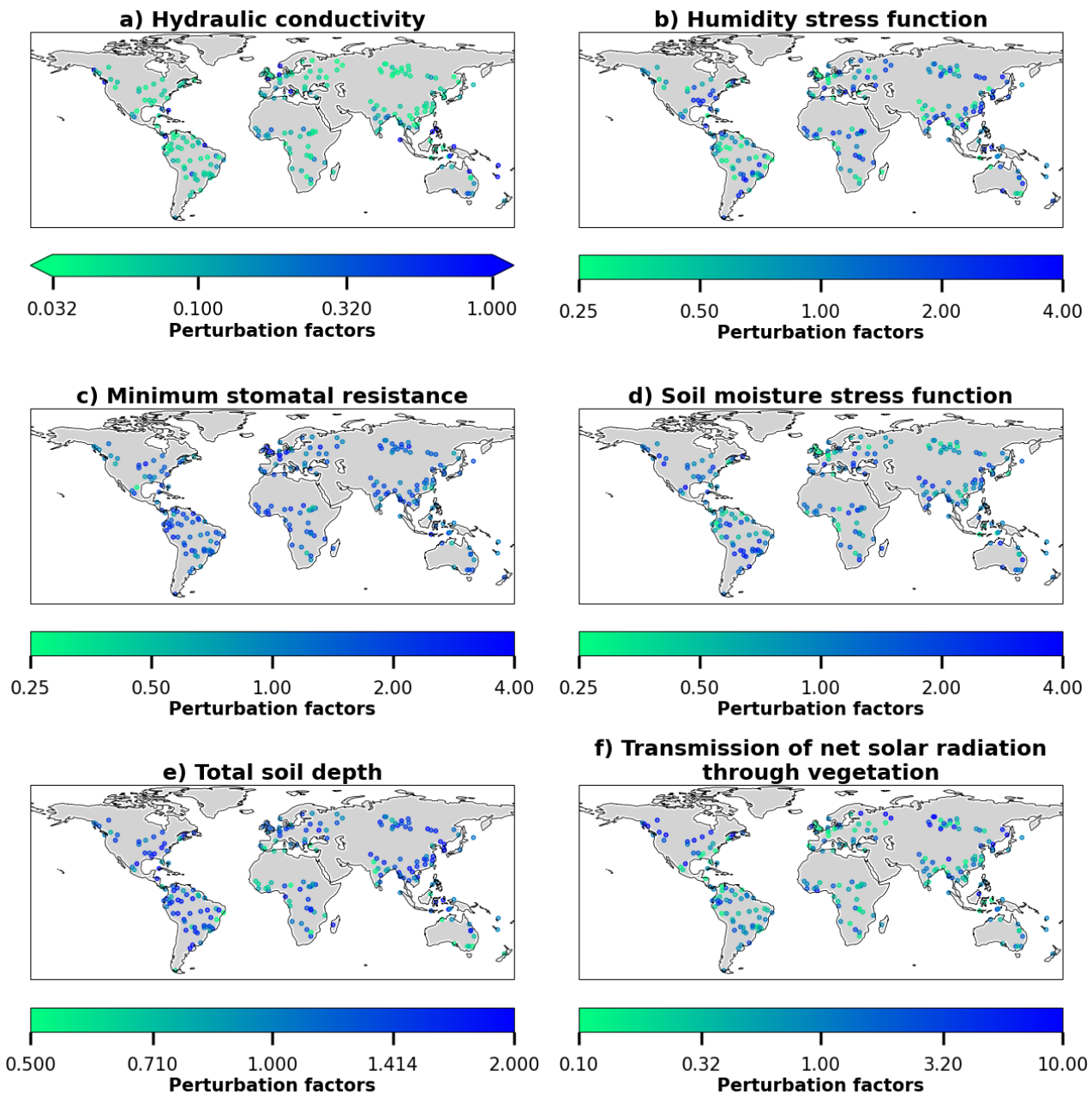


Figure S7. Spatial distribution of the calibrated parameter values in the regional calibration experiment for a) hydraulic conductivity, b) humidity stress function, c) minimum stomatal resistance, d) soil moisture stress function, e) total soil depth and f) transmission of net solar radiation through vegetation.

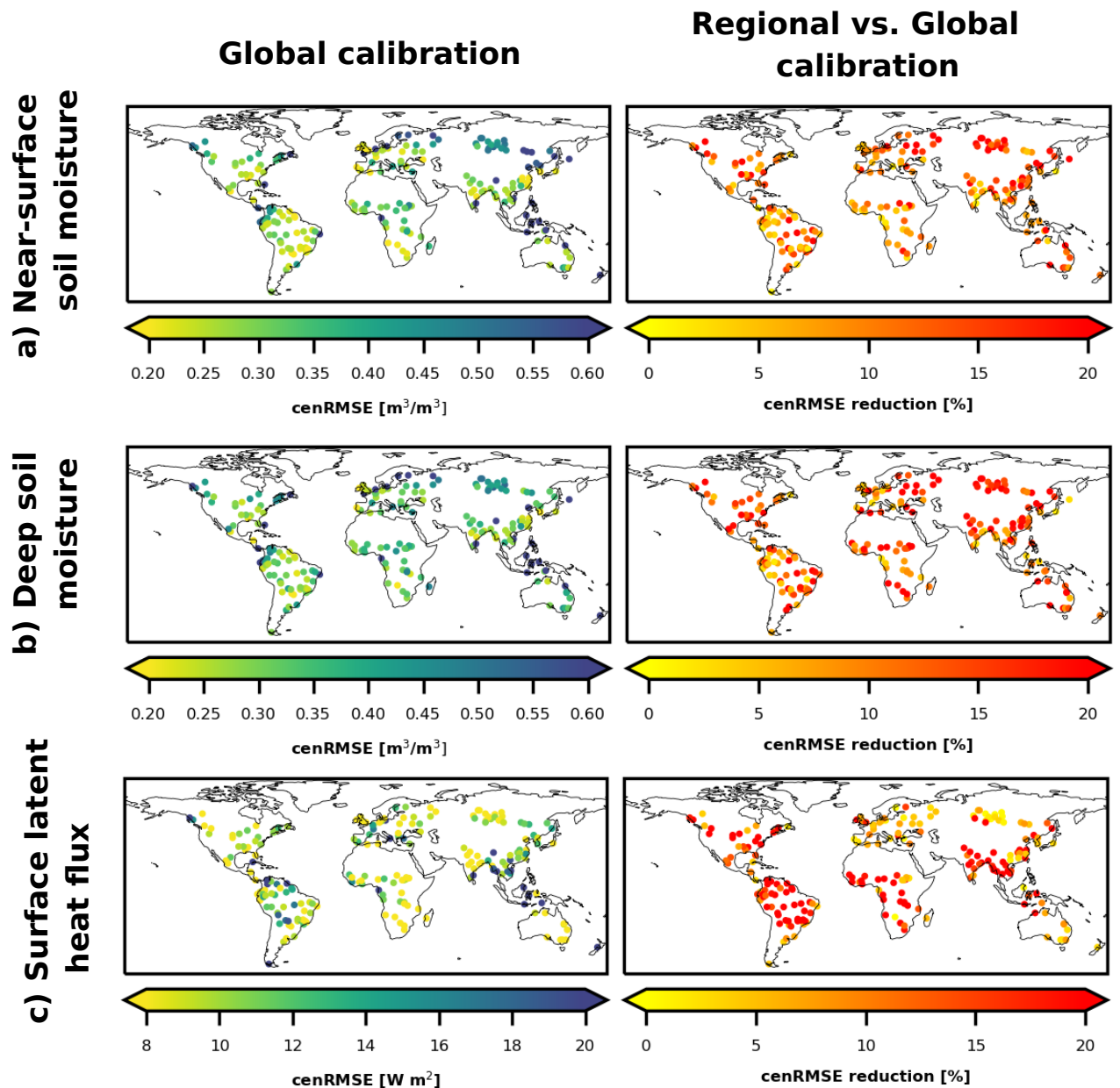


Figure S8. Model performance of the global parameter calibration experiment (left column) and reduction in cenRMSE of the regional parameter calibration experiment with regards to the global calibration experiment (right column) for a) near-surface soil moisture, b) deep soil moisture and c) surface latent heat flux.

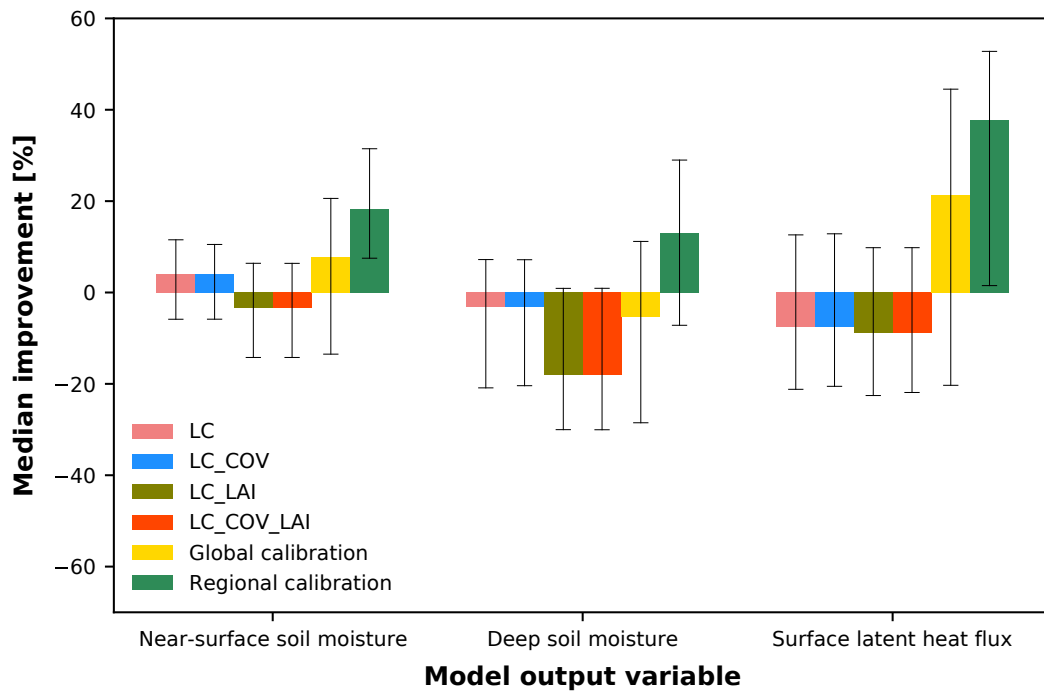
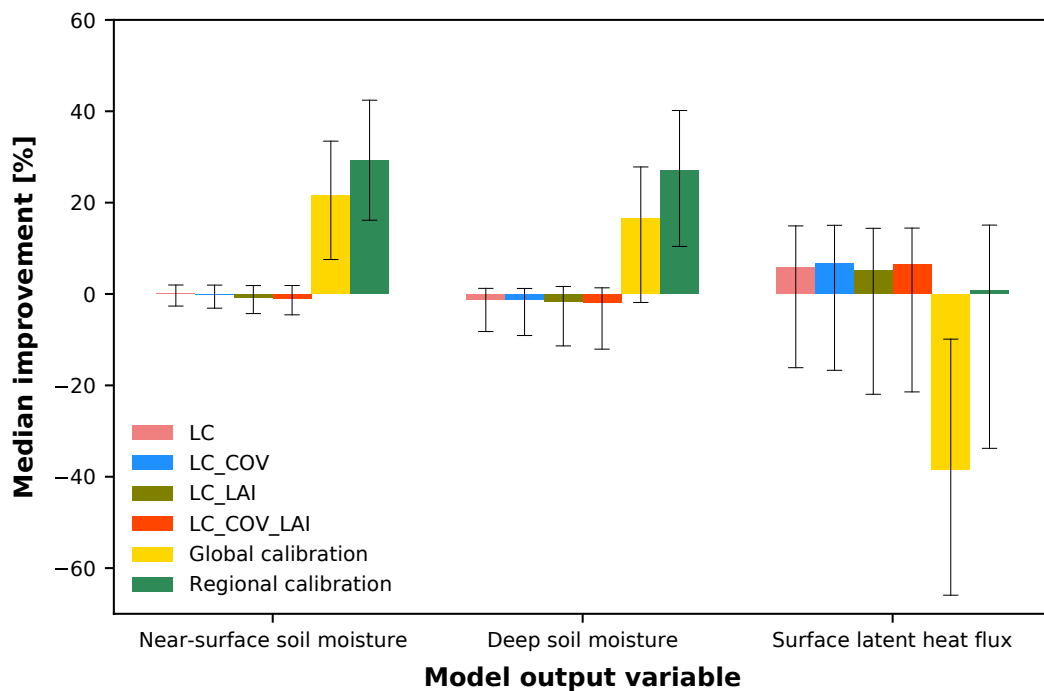
a) Dry grid cells**b) Wet grid cells**

Figure S9. Summary of ECLand performance for each experiment compared to the CONTROL simulation only considering a) dry (\leq first quartile of soil moisture) and b) wet (\geq third quartile of soil moisture) grid cells. The error bars represent the 25th and 75th percentile.

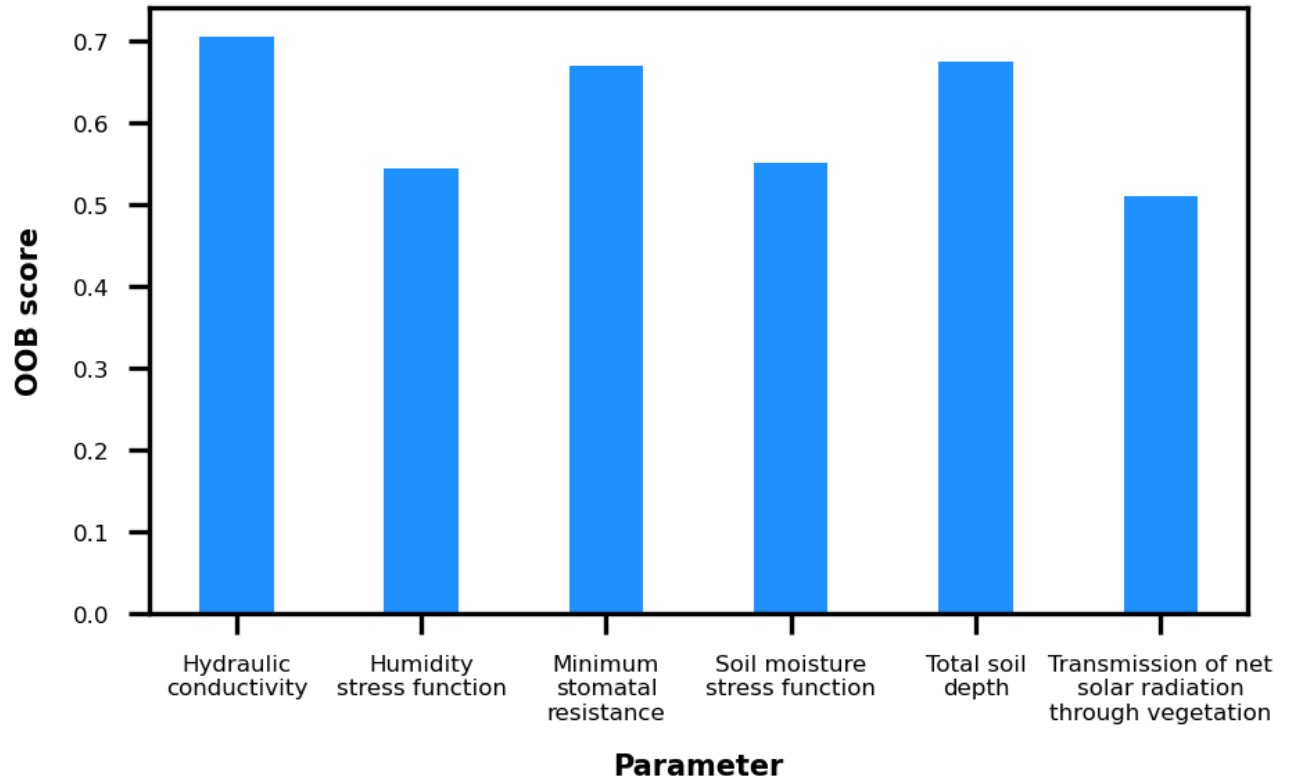


Figure S10. Model performance (OOB estimate of R^2) in the trained RF for the considered six soil and vegetation related model parameters. Higher OOB means the RF can well explain the spatial pattern of model parameters.

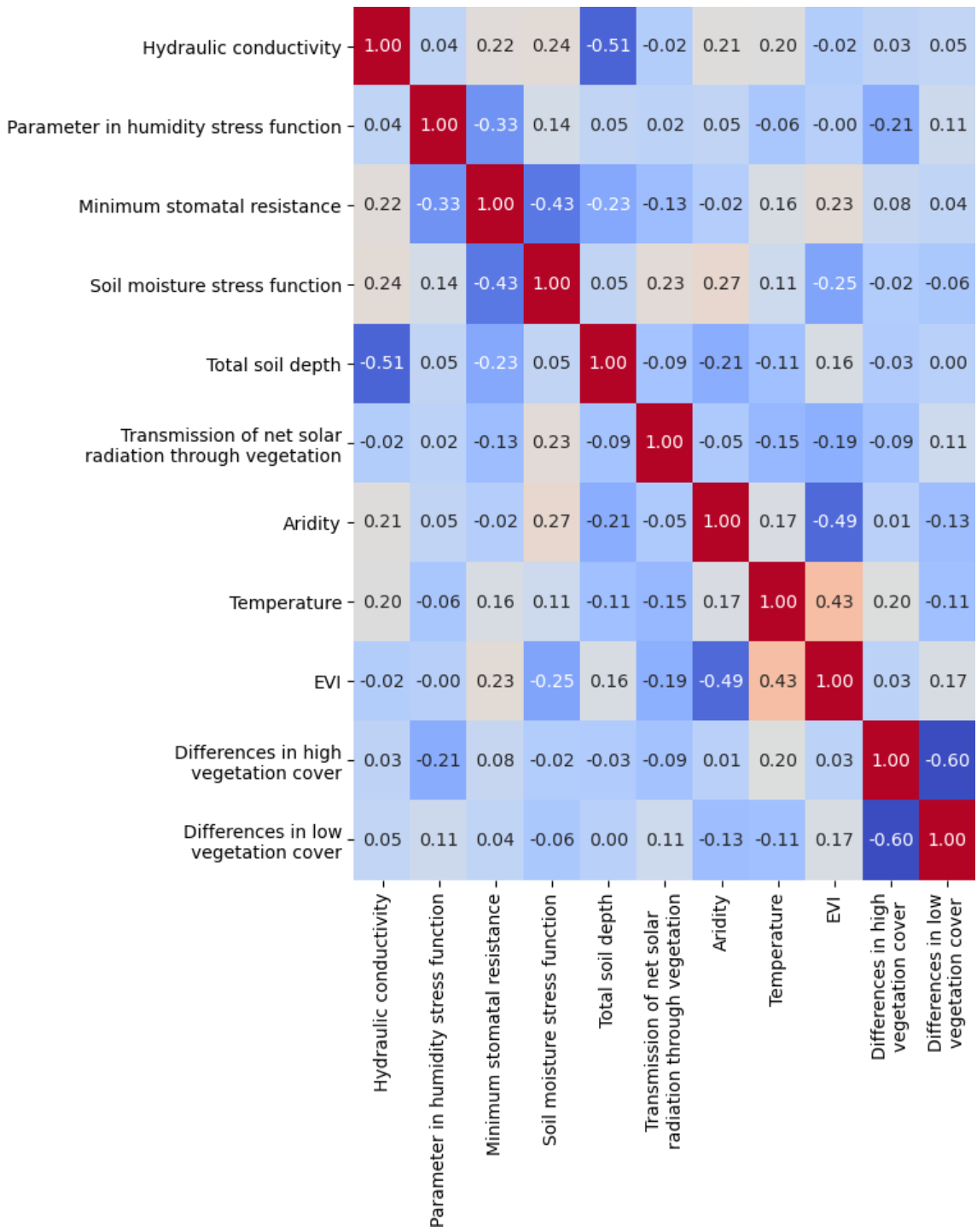


Figure S11. Spearman cross-correlation matrix among the 11 predictors used in the RF models to predict the calibrated parameter values.